Research Article

1

INDONESIAN SCHOLAR SOCIETY

Indones. J. Chem. Stud.
2026, 5(1), 1–7
Available online at journal.solusiriset.com
e-ISSN: 2830-7658; p-ISSN: 2830-778X

Indonesian Journal of Chemical Studies

Enhanced Electromagnetic Absorption of Polyaniline/Fe_3O_4 Nanocomposites in the X-Band Region: Synthesis, Mechanism, and Performance

Annisa Salsabilla[1], Andri Hardiansyah[2], M. Zuhnir Piliang[1], Krisman H.T. Purba[1], Andi Setiono[3], Riri Murniati[1]*

[1]*Department of Physics, Republic of Indonesia Defense University, Bogor 16810, Indonesia*

[2]*Research Center for Nanotechnology Systems, National Research and Innovation Agency (BRIN), Banten 15314, Indonesia*

[3]*Research Center for Photonics, National Research and Innovation Agency (BRIN), Banten 15314, Indonesia*

Received: 17 Aug 2025; Revised: 28 Oct 2025; Accepted: 23 Dec 2025;
Published online: 19 May 2026; Published regularly: 30 Jun 2026

Abstract— PANI can be used as a promising candidate for radar absorbing material. However, the PANI single-composition structure lacks sufficient loss mechanisms, resulting in limited absorption capabilities. This is because PANI is a non-magnetic material, so its microwave absorption properties mostly contributed to dielectric loss. Fe_3O_4 is highly attractive for enhancing the magnetic loss and electromagnetic attenuation. Therefore, the combination of Fe_3O_4 and PANI can improve the impedance matching of the nanocomposites while achieving the demand for lightweight. In this research, PANI/Fe_3O_4 is prepared via chemical oxidative polymerization. The structure and morphology of nanocomposites are characterized using Field Emission Scanning Electron Microscopy with Energy Dispersive X-Ray spectroscopy (FESEM-EDX), X-Ray Diffraction (XRD), and Fourier Transform Infrared spectroscopy (FTIR). The microwave parameters are measured using Vector Network Analyzer (VNA). The maximum reflection loss of PANI/Fe_3O_4 is up to -21.43 dB at 9.2 GHz with its thickness being 2 mm, and its absorption bandwidths exceeding -10 dB are in the range from 8.1 to 10.8 GHz with its thickness being in the range from 2-5 mm. It provides that PANI/Fe_3O_4 nanocomposites have a great potential application for radar absorbing material.

Keywords— *Conductive polymer; Magnetic material; Nanocomposites; Radar absorbing material; Polyaniline.*

1. INTRODUCTION

The utilization of electromagnetic waves-based devices accross various fields, such as electronic devices, communication technologies, as well as Radar systems, have been developed rapidly. Radar works by emitting electromagnetic waves, which are then reflected by objects such as aircraft, and detects the location of the object. On the other hand, a material that can reduce the Radar Cross Section (RCS) of the objects is required in the military field. Recently, Radar Absorbing Materials (RAMs) have received increasing attention among researchers. RAMs are electromagnetic structures used to attenuate incident electromagnetic waves, thereby significantly reducing both reflected and transmitted power [1]. Principally, Radar waves composed of perpendicular magnetic and dielectric field components [2]. Therefore, a RAM should have high electrical and magnetic conductivity to maximize the Radar waves absorption.

In recent years, conductive polymers (CPs) have been widely used as microwave absorber, especially in the range of Radar waves (X-band). A few examples of CPs are Polyacetylene, Polypyrrole, Polyaniline, Polythiophene, etc [3]. CPs have unique characteristics that distinguish them from other polymers, such as tunable or reversible conductivity [4]. Among them, Polyaniline (PANI) has become one of the most extensively investigated CPs because of its remarkable properties, including excellent electrical conductivity, low density, and good chemical stability [5]. The density value of Polyaniline (emeraldine) was 1.329 g/cm^{-3} at 20°C [6]. Additionally, PANI is easy to synthesize and cost-effective, making it a feasible alternative to other CPs [7]. Based on previous study, the conductivity of Polyaniline varied from 0.01-10 S/cm depend on the dopant [8]. Due to the high conductivity, PANI exhibits high dielectric constant and excellent impedance matching. However, the PANI single-composition structure lacks design flexibility and sufficient loss mechanisms, resulting in limited absorption capabilities. Moreover, the impedance mismatch of PANI single-

***Corresponding author**.
Email address: ririmurniati90@gmail.com
DOI: 10.55749/ijcs.v5i1.88

composition leads to reduced microwave absorption performance [9]. Consequently, further enhancement strategies are needed to optimize the microwave absorption performance of PANI. The conductivity of PANI can be improved by compounding it with carbon-based materials, ferrite materials, natural materials, and multicomponent materials [10].

Ferrites, as a magnetodielectric material, exhibit both magnetic loss and dielectric loss mechanisms [11]. Among various ferrites, magnetite (Fe_3O_4) nanoparticles have been thoroughly investigated as microwave absorber due to its cost-effective synthesis, tunable morphology, and strong saturation magnetization [12,13]. Fe_3O_4 can reached high saturation magnetization up to 75.3 emu/g [14]. Furthermore, Fe_3O_4 nanoparticles have unique characteristics such as high magnetic permeability and electrical resistivity, which can effectively reduce the adverse skin effect, thereby enhance the attenuation of electromagnetic waves [15]. The Fe_3O_4 interface generates resonance that leads to increased magnetic loss, thereby enhanced the microwave absorption performance over a wider range [16]. Despite all of the advantages, the broad frequency bandwith of Fe_3O_4 nanoparticles is limited due to their unsuitable dielectric loss [17]. To overcome the above limitations, combining Fe_3O_4 and PANI can achieve better impedance matching without adding significant weight of the nanocomposites.

Recent studies show that integrating lightweight conductive polymer with magnetic nanoparticles could reduced the composite's density and simultaneously enhaced its electromagnetic properties by introducing dielectric loss to the matrix. A previous study revealed that employing hollow structures could produce lightweight Fe_3O_4-based composites with reduced effective density (ρ < 1.0 g/cm^3) [18]. Janem et al. synthesized thin film Fe_3O_4@Polypyrrole nanocomposites with maximum reflection loss (RL) value of 1.5 mm film was -33.8 dB at 11.5 GHz [19]. Zhang et al. also successfully prepared Fe_3O_4/PANI nanocomposite with minimum reflection value of -17.8 dB at 6.22 GHz at the thickness of 5.0 mm [20]. Another dendritic structured Fe_3O_4@PANI composites was synthesized by Luo et al. with the minimum reflection loss (RL) was -53.08 dB at 3.04 GHz with only 1.3 mm thickness. The presence of interface and dipole polarization in the composites leads to enhanced microwave attenuation [21].

In this work, PANI/Fe_3O_4 nanocomposites synthesized via in situ polymerization method and thoroughly evaluated the potential application as RAM. The electromagnetic (EM) waves absorption performance of PANI/ Fe_3O_4 was investigated in the X-band frequency (8-12 GHz) using VNA. The results show that the EM waves absorption performance of PANI/Fe_3O_4 nanocomposites has been enhanced compared with pure Fe_3O_4. The RL_{max} of PANI/Fe_3O_4 is up to -21.43 dB at 9.2 GHz with its thickness being 2 mm and its absorption bandwidths exceeding -10 dB are in the range from 8.1 GHz to 10.8 GHz (2.7 GHz). Furthermore, the nanocomposite' structure and morphology were further analyzed using FESEM, XRD, and FTIR. This study aims to synthesize and characterize PANI/Fe_3O_4 nanocomposites and evaluate their performance as radar absorbing materials in the X-band frequency.

2. EXPERIMENTAL SECTION

2.1. Materials

The materials used in this research were ammonium persulfate (APS), aniline monomer, 1 M hydrochloric acid (HCl), iron (III) chloride ($FeCl_3$), iron (II) chloride ($FeCl_2$), 5 M sodium hydroxide (NaOH), deionized water, ethanol. All of the materials were purchased from Sigma Aldrich, USA.

2.2. Instrumentation

The surface morphology and composition analysis of the samples were observed by FESEM-EDX (ThermoFisher Scientific Apreo 2S, USA). The FTIR spectra of the samples were recorded with Thermoscientific Nicolet iS-10 Fourier Transform Infrared Spectrophotometer (USA). The X-ray diffraction patterns (XRD) were recorded using Cu Kα light source (λ = 1.54056 Å) by SMARTLAB RIGAKU (Japan).

The EM parameters of the samples were recorded in the frequency range of 8-12 GHz by using a vector network analyzer (Anritsu MS2038C VNA Master,USA). The samples were tested using 2, 3, 4, and 5 mm thickness variations. The EM parameters of the samples were measured in the frequency range of 8-12 GHz using waveguide method. The VNA was calibrated for full two-port reflection and transmission measurements at each port.

2.3. Preparation of Fe_3O_4 Nanoparticles

The Fe_3O_4 nanoparticles were synthesized using co-precipitation methods. Briefly, 5.2 g and 2 g of $FeCl_3$ and $FeCl_2$ were dissolved in 75 mL deionized water, respectively. The two solutions were mixed and then 20 mL of 5 M NaOH was added to the mixture. The Fe_3O_4 solution was then washed with ethanol and deionized water. After being washed, the Fe_3O_4 solution was dried in oven at 60°C

2.4. Preparation of PANI/Fe_3O_4 Nanocomposites

In situ polymerization was carried out to synthesize PANI/Fe_3O_4 nanocomposites. First of all, 5 g of APS was dissolved in 20 mL deionized water and 5 mL of aniline was mixed with 70 mL of 1 M HCl. The Fe_3O_4 powder was then added to the aniline solution. After that, the APS solution was added to the mixture gradually. The mixture was put in an ice bath and stirred for 4 h. The PANI/Fe_3O_4 solution was then washed with ethanol and deionized water. After cleansing, the PANI/Fe_3O_4 solution was dried in oven at 60°C. Furthermore, the powder was filtered with 400 mesh.

The schematic illustration of the nanocomposites fabrication are shown in **Fig. 1**.

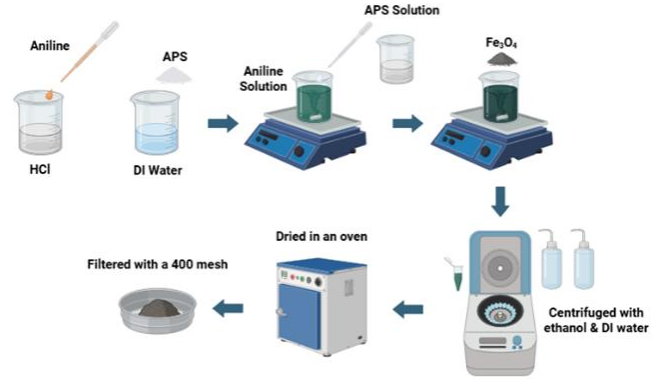

Fig. 1 Schematic illustration of PANI/Fe_3O_4 nanocomposites fabrication

2.5. Formation Mechanism of PANI/Fe_3O_4

Fig. 2 presented the formation mechanism of PANI/Fe_3O_4 nanocomposites. The formation of PANI/Fe_3O_4 nanocomposites is typically achieved through an in situ oxidative polymerization mechanism, in which the aniline monomers are polymerized in the presence of Fe_3O_4 nanoparticles. Initially, aniline is protonated in the acidic medium (HCl), which promotes adsorptions onto the surface of Fe_3O_4. Protonation of PANI by HCl results in the donation of protons to the nitrogen atoms, converting from emeraldine base to emeraldine salt form and enhancing conductivity. The introduction of ammonium persulfate (APS) caused aniline to oxidize and form radical cations. The radical cations subsequently undergo coupling reactions, initiating the oxidative polymerization process. Fe_3O_4 acts as the nucleation sites, directing the growth of polyaniline chains and enabling the formation of a polymer shell. The resulting nanocomposites exhibit a core-shell structure of PANI in the emeraldine salt phase [22,23].

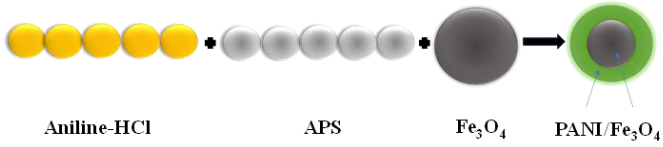

Fig. 2 Formation mechanism of PANI/Fe_3O_4 nanocomposites

3. RESULT AND DISCUSSION

3.1. FESEM-EDX

FESEM images of the Fe_3O_4 and PANI/Fe_3O_4 nanocomposites are depicted in **Fig. 3**. As it could be seen in **Fig. 3(a),** it is obvious that Fe_3O_4 nanoparticles possess a spherical shape. The Fe_3O_4 nanoparticles exhibit a uniform size distribution. From **Fig. 3(b),** the coral-like structure of PANI could not be seen because polyaniline nucleation on the surface of the nanoparticles. It confirmed the success of synthesis process of PANI/Fe_3O_4 nanocomposites.

Table 1 shows the EDX analysis of the Fe_3O_4 and PANI/Fe_3O_4 nanocomposites. The weight percent of iron and oxygen in Fe_3O_4 are 76.6 and 23.4, respectively. In the EDX analysis of PANI/Fe_3O_4, the peaks of carbon, nitrogen, iron, and oxygen can be clearly seen, confirming the formation of the nanocomposites. The appearance of chlorine peaks are due to the presence of HCl as the dopant.

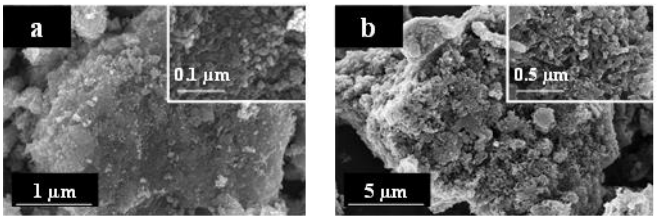

Fig. 3 FESEM images of (a) Fe_3O_4 and (b) PANI/Fe_3O_4

Table 1. Elemental composition of synthesized Fe_3O_4 and PANI/Fe_3O_4 nanocomposites

Materials	Elements	Atomic %	Weight %
Fe_3O_4	Fe	48.4	76.6
	O	51.6	23.4
PANI/Fe_3O_4	N	15.9	14.5
	Cl	3.0	6.8
	C	50.0	39.1
	O	28.2	29.4
	Fe	2.8	10.2

3.2. FTIR

Fig. 4 indicates the FTIR absorption spectra of PANI, Fe_3O_4, and PANI/Fe3O4 nanocomposites in the range of wavenumber from 4000 to 500 cm^{-1}. For PANI nanocomposites, the peaks at 1564.5 and 1494.1 cm^{-1} are due to C=C and C=N stretching vibrations of benzenoid and quinoid rings, respectively. The band at 1293.1 cm^{-1} is attributed to C-N stretching vibrations of aromatic amine. The strong peaks at 875.1, 742, and 682.2 cm^{-1} are assigned to group of C-H bending. The band at 3120.4 cm^{-1} corresponds to N-H stretching vibration of secondary amine.

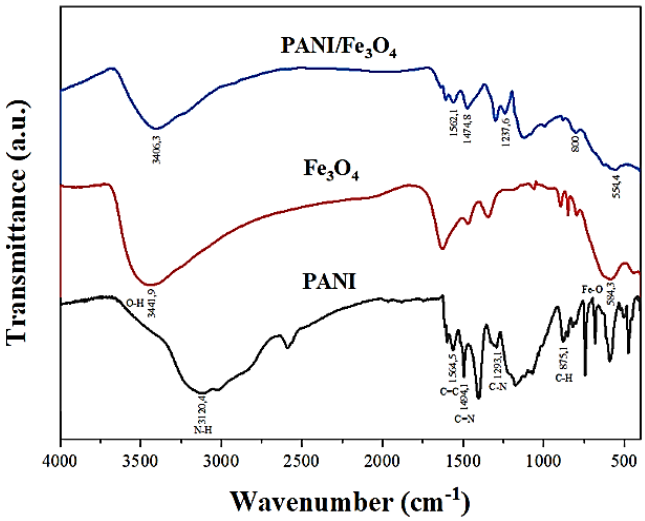

Fig. 4 FTIR spectra of PANI, Fe_3O_4, and PANI/Fe_3O_4

A characteristic absorption band is observed at 584.3 cm^{-1} due to the stretching vibration of Fe-O bonds in the Fe_3O_4 spectrum (**Table 2**). This band value closely resembles the previous study [24]. The observed absorption band centered at 3441.9 cm^{-1} corresponds to O-H stretching vibration attached to the Fe_3O_4 surface, as reported in the early work [25].

Table 2. Shift of wavenumber of the functional groups in FTIR spectra

Functional Groups	Wavenumber (cm^{-1})		
	PANI	Fe_3O_4	PANI/Fe_3O_4
N-H	3120.4	-	-
C=C	1564.5	-	1562.1
C=N	1494.1	-	1474.8
C-N	1293.1	-	1237.6
C-H	875.1	-	800
O-H	-	3441.9	3406.3
Fe-O	-	584.3	554.4

The FTIR absorption spectra of PANI/Fe_3O_4 nanocomposites appear slight shift toward high frequency. This spectral shift is because of the existence of physical forces between PANI and Fe_3O_4 [26]. The appearance of a weak peak at 554.4 cm^{-1} (due to Fe-O bond) shows the presence of Fe_3O_4 in the PANI/Fe_3O_4 nanocomposites. All of the characteristic peaks of PANI are found, proving that the Fe_3O_4 nanoparticles are successfully dispersed into PANI/Fe_3O_4 nanocomposites. The spectral shift towards lower wavelengths indicating blue shift.

3.3. XRD

The XRD patterns of Fe_3O_4 nanoparticles and PANI/Fe_3O_4 nanocomposites are shown in **Fig. 5**. The characteristic diffraction peaks of Fe_3O_4 nanoparticles appeared at 2θ = 35.6°, 62.8°, 30.2°, 57.2°, 43.2°, and 53.6° correspond to (311), (440), (220), (511), (400), and (422) crystal planes, respectively. The positions of the diffraction peak and the relative intensities of the plane diffraction peak are matched in good agreement with the ICSD 98-015-8744. Therefore, the crystal system of Fe_3O_4 nanoparticles is cubic Fd-3m space group with face-centered cubic (FCC) lattice and inverse spinel as the crystal structure. The broad diffraction band from 10° to 20° indicated the amorphous structure of PANI. Furthermore, these results indicated that Fe_3O_4 nanoparticles are still present in the nanocomposites structure.

The crystallite size of the nanocomposites can be calculated using the Scherrer equation [27]:

$$D = k\lambda/\beta\cos\theta \quad (1)$$

where k is integer (0.9), λ is X-Ray wavelength (0.154 nm), β is full width at half-maximum (FWHM) (Rad), and θ is Bragg-diffraction angle or peak positions in radian (degree). From the calculation, the obtained average particle diameter of Fe_3O_4 nanoparticles is approximately 11 nm, whereas the average particle diameter of the PANI/Fe_3O_4 nanocomposites is around 21 nm. This increase in particle size is caused by the PANI nucleation on the surface of Fe_3O_4. The obtained values are similar to that reported in previous work [28].

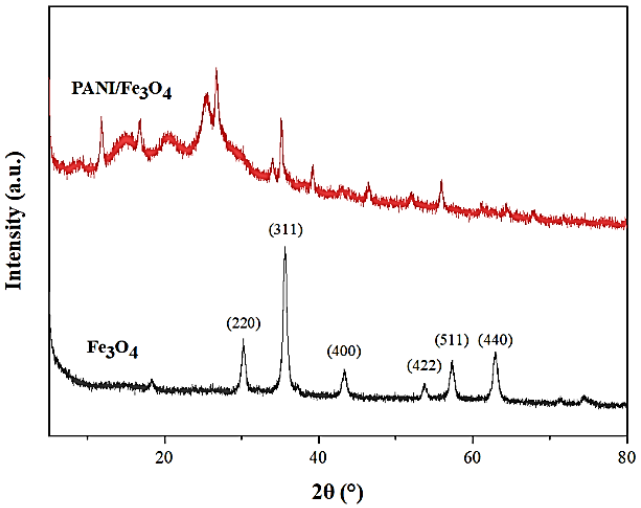

Fig. 5 XRD pattern of Fe_3O_4, and PANI/Fe_3O_4

3.4. VNA

According to the transmission line theory, the value of RL was calculated using the equation summarized below [29]:

$$Z_{in} = Z_0\sqrt{\frac{\mu_r}{\varepsilon_r}}\tanh\left[j\left(\frac{2\pi fd}{c}\sqrt{\frac{\mu_r}{\varepsilon_r}}\right)\right] \quad (2)$$

$$R_L = 20\log\left|\frac{Z_{in}-Z_0}{Z_{in}+Z_0}\right| \quad (3)$$

$$Z_0 = \sqrt{\frac{\mu_0}{\varepsilon_0}} \approx 377\Omega \quad (4)$$

where f is the microwave frequency, d is the material thickness, c is the speed of light, ε_0 and μ_0 are the permittivity and permeability of the free space, ε_r and μ_r are the relative complex permittivity and permeability, meanwhile Z_{in} and Z_0 are the impedances of the absorber and the free space, respectively. If the RL value obtained is less than -15 dB, it indicates that 96.9% of the radar waves are absorbed by the nanocomposites. Meanwhile, if the RL value obtained is less than -20 dB, then the absorbed wave is almost 99.0% [30].

Fig. 6 presents the RL values of PANI/Fe_3O_4 nanocomposites at different thickness versus frequency in the range of 8-12 GHz. The appearance of absorption valleys represented the amount of radar waves were absorbed by the material. As can be seen, the thickness of an absorber has no significant influence on either the frequency of reflection loss or intensity. The maximum RL value obtained is -21.43 dB at 9.2 GHz with a thickness of 2 mm. Meanwhile, the effective absorption bandwidth (EAB) over -10 dB ranged from 8.1-10.8 GHz (2.7 GHz). It means that the wave being absorbed by the material is almost 99.0%. This result showed an improvement in PANI/Fe_3O_4 compared to single PANI, as reported in previous study [31]. For the thickness of 3

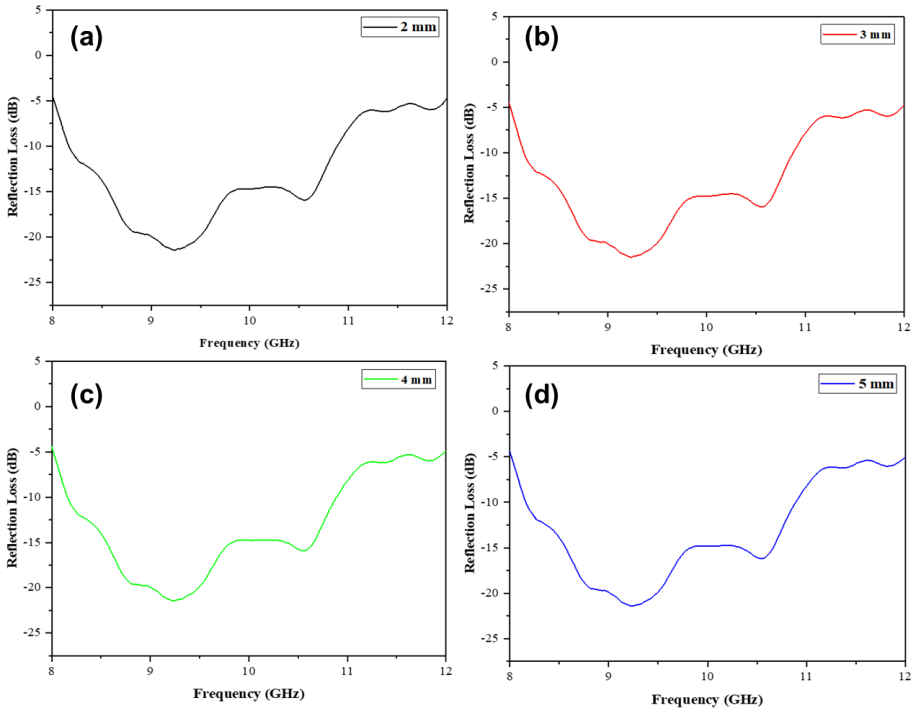

Fig. 6 RL curves of PANI/Fe_3O_4 nanocomposites with variation of thickness: (a) 2 mm, (b) 3 mm, (c) 4 mm, and (d) 5 mm

Table 3. Comparison of reflection loss of PANI/Fe3O4 with other reported similar composites

Materials	RL_{max} (dB)	Frequency (GHz)	Thickness (mm)	EAB (GHz)	References
Ce-BaM ($Ba_{0.8}Ce_{0.2}Fe_{12}O_{19}$)/PANI	-21.6	14.12	1.58	3.88	[32]
$Ba_{0.9}La_{0.1}Fe_{12}O_{19}$/PANI	-13.2	12.8	1.75	2.52	[33]
$CoFe_2O_4$/PANI	-22.3	11.0-17.1	2.5	6.1	[34]
PANI/Fe_3O_4	-21.43	9.2	2	2.7	This work
PANI/Fe_3O_4	-21.48	9.2	3	2.7	This work
PANI/Fe_3O_4	-21.44	9.2	4	2.7	This work
PANI/Fe_3O_4	-21.42	9.2	5	2.7	This work

mm, although the maximum RL value achieved is up to -21.48 dB slightly higher than that of the thickness of 2 mm, it cannot satisfy the requirement of the thin thickness for RAM [35]. These results indicate that PANI/Fe_3O_4 exhibits improved reflection loss compared to single-composition PANI, consistent with finding from previous study [36].

To evaluate the performance of the synthesized PANI/Fe_3O_4 nanocomposites, their reflection loss values were compared to those of similar reported composites listed in **Table 3**. According to the loss mechanism depicted in **Fig. 7**, the PANI/Fe_3O_4 nanocomposites have two kinds of loss mechanism: the dielectric loss and the magnetic loss. PANI, as a conducting polymer, primarily contributes to dielectric loss, whereas Fe_3O_4, as a magnetic material, mainly contributes to magnetic loss.

When incident waves interact with the nanocomposites, the polarons and bipolarons of PANI facilitate charge transport and hopping conductivity, thereby dissipating the electromagnetic energy into heat. The dielectric loss is further enchanced by the interfacial polarization at the nanocomposites interfaces. Simultaneously, the magnetic dipoles of Fe_3O_4 attempt to align with the applied field frequency by absorbing the magnetic component, leading to the dissipation of magnetic energy as thermal energy. The synergistic effect of dielectric and magnetic loss improves impedance matching of the material, allowing more electromagnetic waves to penetrate into the material for better attenuation. This results indicated PANI/Fe_3O_4 as a promising candidate for radar absorbing material [37].

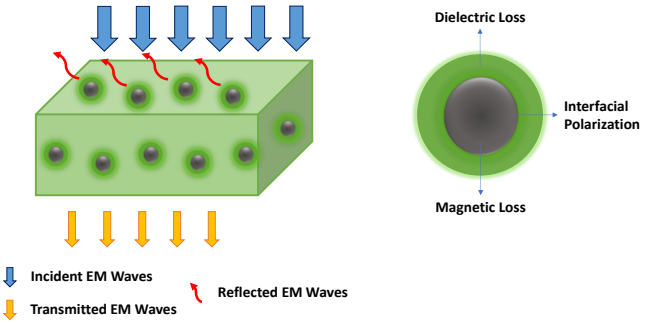

Fig. 7 Schematic illustration of the absorption mechanism for PANI/Fe_3O_4 nanocomposites

4. CONCLUSION

The PANI/Fe_3O_4 nanocomposites have been successfully synthesized by in situ polymerization methods. With Fe_3O_4 nanoparticles as the nucleation sites of PANI, it shows that the nanocomposites have a core/shell structure. The PANI/Fe_3O_4 nanocomposites show enhanced microwave absorption properties due to the introduction of dielectric loss and magnetic loss that leads to the improvement of impedance matching. A maximum reflection loss of -21.43 dB at 9.2 GHz has been obtained with 2 mm thickness. Therefore, the PANI/Fe_3O_4 nanocomposites can be a promising radar absorbing material (RAM) with lightweight, thin thickness, and strong absorption properties. However, further study is required to optimize the synthesis process, investigate long-term stability, and evaluate real-environment performance.

5. AUTHOR'S DECLARATION

5.1. Supporting Information

There is no supporting information in this paper. The data supporting this research's findings are available on request from the corresponding author (RM).

5.2. Acknowledgements

The authors acknowledge the support from Nanocarbon Functional Reseach Group, Research Center for Nanotechnology Systems, National Research and Innovation Agency (BRIN), Tangerang Selatan, Indonesia.

5.3. Conflict of Interest

There was no conflict of interest in this study.

5.4. Author Contributions

AS, AH, MZP, KHTP, AS, and RM were evenly contributed in this research. This study was designed and conducted by AS, AH, and KHTP while AS was the manager of the characterizations. All authors were agreed to the final version of this manuscript.

5.5. AI Statement

ChatGPT was utilize to enhance the clarity, grammar, and overall readability of this manuscript. All technical content, data interpretation, and conclusion were solely developed and verified by the authors. The final version of the manuscript was thoroughly reviewed to ensure accuracy, coherence, and aligment with the study's findings.

6. REFERENCES

[1] Plyushch, A., Macutkevic, J., Svirskas, S., Banys, J., Plausinaitiene, V., Bychanok, D., Maksimenko, S.A., Selskis, A., Sokal, A., Lapko, K.N. and Kuzhir, P.P. 2019. Silicon carbide/phosphate ceramics composite for electromagnetic shielding applications: Whiskers vs particles. *Appl. Phys. Lett.* 114(18). 183105. doi: https://doi.org/10.1063/1.5093421.

[2] Bhattacharya, P., Sahoo, S. and Das, C.K. 2013. Microwave absorption behaviour of MWCNT based nanocomposites in X-band region. *Express Polym. Lett.* 7(3). 212–223. doi: https://doi.org/10.3144/expresspolymlett.2013.20.

[3] Thomas, P., Abdulhakim, L.V., Pushkaran, N.K. and Karuvandi, A.C. 2020. Wideband radar absorbing structure using polyaniline-graphene nanocomposite. *C.* 6(4). 72. doi: https://doi.org/10.3390/c6040072.

[4] Kumar, V., Yokozeki, T., Goto, T., Takahashi, T., Dhakate, S.R. and Singh, B.P. 2017. Irreversible tunability of through-thickness electrical conductivity of polyaniline-based CFRP by de-doping. *Compos. Sci. Technol.* 152. 20–26. doi: https://doi.org/10.1016/j.compscitech.2017.09.005.

[5] Majeed, A.H., Mohammed, L.A., Hammoodi, O.G., Sehgal, S., Alheety, M.A., Saxena, K.K., Dadoosh, S.A., Mohammed, I.K., Jasim, M.M. and Salmaan, N.U. 2022. A review on polyaniline: synthesis, properties, nanocomposites, and electrochemical applications. *Int. J. Polym. Sci.* 2022(1). 9047554. doi: https://doi.org/10.1155/2022/9047554.

[6] Stejskal, J. and Gilbert, R.G. 2002. Polyaniline. Preparation of a conducting polymer (IUPAC technical report). *Pure Appl. Chem.* 74(5). 857-867. doi: https://doi.org/10.1351/pac200274050857.

[7] Baker, C.O., Huang, X., Nelson, W. and Kaner, R.B. 2017. Polyaniline nanofibers: broadening applications for conducting polymers. *Chem. Soc. Rev.* 46(5). 1510-1525. doi: https://doi.org/10.1039/C6CS00555A.

[8] Bednarczyk, K., Matysiak, W., Tański, T., Janeczek, H., Schab-Balcerzak, E. and Libera, M. 2021. Effect of polyaniline content and protonating dopants on electroconductive composites. *Sci. Rep.* 11(1). 7487. doi: https://doi.org/10.1038/s41598-021-86950-4.

[9] Su, X., Liu, Y., Liao, Z., Bi, Y., Ma, M., Chen, Y., Ma, Y., Wan, F. and Chung, K.L. 2022. Recent progress of polyaniline-based composites in the field of microwave absorption. *Synth. Met.* 291. 117190. doi: https://doi.org/10.1016/j.synthmet.2022.117190.

[10] Lin, T., Yu, H., Wang, L., Fahad, S., Khan, A., Naveed, K.U.R., Haq, F., Nazir, A. and Amin, B.U. 2021. A review of recent advances in the preparation of polyaniline-based composites and their electromagnetic absorption properties. *J. Mater. Sci.* 56(9). 5449-5478. doi: https://doi.org/10.1007/s10853-020-05631-1.

[11] Mu, Y., Ma, Z.H., Liang, H.S., Zhang, L.M. and Wu, H.J. 2022. Ferrite-based composites and morphology-controlled absorbers. *Rare Met.* 41(9). 2943-2970. doi: https://doi.org/10.1007/s12598-022-02045-7.

[12] Wang, X., Xing, X., Zhu, H., Li, J. and Liu, T. 2023. State of the art and prospects of Fe_3O_4/carbon microwave absorbing composites from the dimension and structure perspective. *Adv. Colloid Interface Sci.* 318. 102960. doi: https://doi.org/10.1016/j.cis.2023.102960.

[13] Qoidah, S.N., Taufiq, A., Mufti, N., Sunaryono, S., Hidayat, N., Handoko, E., Alaydrus, M. and Amrillah, T. 2024. Fe_3O_4/MWCNT/TiO_2 nanocomposites as excellent microwave absorber material. *J. Alloys Compd.* 970. 172590. doi: https://doi.org/10.1016/j.jallcom.2023.172590.

[14] Hu, P., Kang, L., Chang, T., Yang, F., Wang, H., Zhang, Y., Yang, J., Wang, K.S., Du, J. and Yang, Z. 2017. High saturation magnetization Fe_3O_4 nanoparticles prepared by one-step reduction method in autoclave. *J. Alloys Compd.* 728. 88-92. doi: https://doi.org/10.1016/j.jallcom.2017.08.290.

[15] Liu, Y., Chen, Z., Xie, W., Song, S., Zhang, Y. and Dong, L. 2019. In-situ growth and graphitization synthesis of porous Fe3O4/carbon fiber composites derived from biomass as lightweight microwave absorber. *ACS Sustain. Chem. Eng.* 7(5). 5318-5328. doi: https://doi.org/10.1021/acssuschemeng.8b06339.

[16] Li, N., Huang, G.W., Li, Y.Q., Xiao, H.M., Feng, Q.P., Hu, N. and Fu, S.Y. 2017. Enhanced microwave absorption performance of coated carbon nanotubes by optimizing the Fe_3O_4 nanocoating structure. *ACS Appl. Mater. Interfaces.* 9(3). 2973-2983. doi: https://doi.org/10.1021/acsami.6b13142.

[17] Gang, Q., Akhtar, M.N. and Boudaghi, R. 2021. Development of high-efficient double layer microwave absorber based on Fe_3O_4/carbon fiber and Fe_3O_4/rGO. *J. Magn. Magn. Mater.* 537. 168181. doi: https://doi.org/10.1016/j.jmmm.2021.168181.

[18] Sun, L., Li, Q., Wang, W., Pang, J. and Zhai, J. 2011. Synthesis

of magnetic and lightweight hollow microspheres/polyaniline/Fe_3O_4 composite in one-step method. *Appl. Surf. Sci.* 257(23). 10218-10223. doi: https://doi.org/10.1016/j.apsusc.2011.07.024.

[19] Janem, N., Azizi, Z.S. and Tehranchi, M.M. 2021. Microwave absorption and magnetic properties of thin-film Fe_3O_4@ polypyrrole nanocomposites: The synthesis method effect. *Synth. Met.* 282. 116948. doi: https://doi.org/10.1016/j.synthmet.2021.116948.

[20] Zhang, D., Chen, H. and Hong, R. 2019. Preparation and conductive and electromagnetic properties of Fe_3O_4/PANI nanocomposite via reverse in situ polymerization. *J. Nanomater.* 2019(1). 7962754. doi: https://doi.org/10.1155/2019/7962754.

[21] Luo, X., Li, H., Deng, D., Zheng, L., Wu, Y., Luo, W., Zhang, M. and Gong, R. 2022. Preparation and excellent electromagnetic absorption properties of dendritic structured Fe_3O_4@PANI composites. *J. Alloys Compd.* 891. 161922. doi: https://doi.org/10.1016/j.jallcom.2021.161922.

[22] Toroń, B., Das, T.K., Kozioł, M., Szperlich, P. and Kępińska, M., 2025. Impact of hydrochloric acid doping on polyaniline conductivity and piezoelectric performance in polyaniline/bismuth oxyiodide nanocomposites. *Compos. Part B Eng.* 289. 111960 doi: https://doi.org/10.1016/j.compositesb.2024.111960.

[23] Ćirić-Marjanović, G. 2013. Recent advances in polyaniline research: Polymerization mechanisms, structural aspects, properties and applications. *Synth. Met.* 177. 1-47. doi: https://doi.org/10.1016/j.synthmet.2013.06.004.

[24] Elashmawi, I.S. and Alhusaiki-Alghamdi, H.M. 2024. Fabrication, characterization, spectroscopic, and magnetic properties of polyaniline/magnetite (PANi/Fe_3O_4) nanocomposites. *Opt. Quantum Electron.* 56(7). 1090. doi: https://doi.org/10.1007/s11082-024-06843-4.

[25] Gholivand, M.B., Yamini, Y., Dayeni, M. and Seidi, S. 2015. Removal of methylene blue and neutral red from aqueous solutions by surfactant-modified magnetic nanoparticles as highly efficient adsorbent. *Environ. Prog. Sustain. Energy.* 34(6). 1683-1693. doi: https://doi.org/10.1002/ep.12174.

[26] Muhammad, A., Shah, A.U.H.A., Bilal, S. and Rahman, G., 2019. Basic Blue dye adsorption from water using Polyaniline/Magnetite (Fe_3O_4) composites: Kinetic and thermodynamic aspects. *Materials.* 12(11). 1764. doi: https://doi.org/10.3390/ma12111764.

[27] Rasendriya, A.B., Hardiansyah, A., Amalia, G.R., Rahmadtullah, I., Setiono, A., Piliang, M.Z., & Renta, H. 2025. Fabrication and characterization of graphene nanoplatelets/zinc oxide nanocomposites as a military radar absorbing material. *Indones. J. Chem. Stud.* 4(1) 28–34. doi: https://doi.org/10.55749/ijcs.v4i1.69.

[28] De Araújo, A.C.V., De Oliveira, R.J., Júnior, S.A., Rodrigues, A.R., Machado, F.L.A., Cabral, F.A.O. and De Azevedo, W.M. 2010. Synthesis, characterization and magnetic properties of polyaniline-magnetite nanocomposites. *Synth. Met.* 160(7-8). 685-690. doi: https://doi.org/10.1016/j.synthmet.2010.01.002.

[29] Ruiz-Perez, F., López-Estrada, S.M., Tolentino-Hernández, R.V. and Caballero-Briones, F. 2022. Carbon-based radar absorbing materials: A critical review. *J. Sci. Adv. Mater. Devices.* 7(3).100454. doi: https://doi.org/10.1016/j.jsamd.2022.100454.

[30] Idris, F.M., Hashim, M., Abbas, Z., Ismail, I., Nazlan, R. and Ibrahim, I.R. 2016. Recent developments of smart electromagnetic absorbers based polymer-composites at gigahertz frequencies. *J. Magn. Magn. Mater.* 405. 197-208. doi: https://doi.org/10.1016/j.jmmm.2015.12.070.

[31] Shi, Y., Chen, J., Dai, J. and Qiu, J. 2020. Frequency selective absorbing property of nanoring-shaped polyaniline with broadband absorption. *J. Mater. Sci. Mater. Electron.* 31(4). 3622-3630. doi: https://doi.org/10.1007/s10854-020-02917-7.

[32] Liu, X., Ji, R., Yang, M., Chen, W., Chen, H., Song, X., Liu, J., Zhang, M. and Zhang, L. 2023. Facilitating enhanced microwave absorption properties of barium hexaferrite/polyaniline composites based on tunable interfacial polarization by rare earth doping. *J. Alloys Compd.* 937. 168391. doi: https://doi.org/10.1016/j.jallcom.2022.168391.

[33] Tran, N., Lee, M.Y., Jeong, W.H., Phan, T.L., Tuan, N.Q. and Lee, B.W. 2021. Thickness independent microwave absorption performance of La-doped $BaFe_{12}O_{19}$ and polyaniline composites. *J. Magn. Magn. Mater.* 538. 168299. doi: https://doi.org/10.1016/j.jmmm.2021.168299.

[34] Chen, P., Jiang, L.W., Yang, S.S., Chen, H.B., He, J., Wang, Y. and An, J. 2020. Facile synthesis and microwave-absorption properties of organic–inorganic $CoFe_2O_4$/polyaniline nanocomposites with embedded structure. *J. Nanosci. Nanotechnol.* 20(3). 1756-1764. doi: https://doi.org/10.1166/jnn.2020.17150.

[35] Sinde, D.D., Babu, V. and Khandal, S.V. 2022. A Review on types of radar absorbing materials. *Shanlax Int. J. Manag.* 9. 122-127. doi: https://doi.org/10.34293/management.v9iS1-Mar.4901.

[36] Zhang, Y., Liu, J., Zhang, Y., Liu, J. and Duan, Y. 2017. Facile synthesis of hierarchical nanocomposites of aligned polyaniline nanorods on reduced graphene oxide nanosheets for microwave absorbing materials. *RSC Adv.* 7(85). 54031-54038. doi: https://doi.org/10.1039/c7ra08794b.

[37] Ruchi, Gupta, V., Dalal, R. and Goyal, S.L., 2024. Electromagnetic interference shielding performance of in-situ polymerized PANI/Fe_3O_4 nanocomposites in X-band frequency range. *Polym. Bull.* 81(6). 5155-5178. doi: https://doi.org/10.1007/s00289-023-04950-y.